

## Thermal Combustion Characteristics of Stabilized Swirl Burner for Prevaporized Partially Premixed Flames

Hassan. S. Mohamed<sup>3</sup>, H. A. Moneib<sup>1</sup>, H. M. El-Batsh<sup>2</sup>, A. M. A. Attia<sup>2</sup>, and R. M. Elzoherry<sup>2</sup>

<sup>1</sup>Mechanical Power Engineering Department, Faculty of Engineering, Mattaria, Helwan University, Egypt.

<sup>2</sup>Mechanical Engineering Department, Benha Faculty of Engineering, Benha University, Egypt.

<sup>3</sup> Atomic Energy Authority, Egypt.

Corresponding author: [ansaam.76@yahoo.com](mailto:ansaam.76@yahoo.com)

### Abstract

This study aims to investigate the effect of combustion of a mixture of biodiesel / A-1 jet fuel on the flame characteristics in the combustion chamber. Esterification of waste cooking oil (WCO) to produce biodiesel (WCOME) fuel was carried out using ultrasonicator to reduce production time. To maintain the flame stability, a swirl burner having a swirl number equal to (SN=0.55) was used to form a central vortex zone. The evaporated fuel was pre-mixed with air preheated to a temperature of 250°C at equivalence ratio ( $\Phi = 0.75$ ) at all operating conditions. The mixture of B5 and B10 (5% biodiesel and 10% by volume with Jet A-1) is pre-evaporated and pre-mixed with air before being fed into a cylindrical combustion chamber of inner diameter ( $D = 150$  mm) and length ( $L = 500$  mm). Under all operating conditions the temperature of the pre-mixed fuel/air mixture remains constant at 250°C and a lean equivalent ratio ( $\Phi = 0.75$ ). The effects of excess air ( $\lambda = 33\%$ ), equivalence ratio ( $\phi=0.75$ ) and , preheated air temperature ( $T \geq 250$  C°) , prevaporized fuel with fuel nozzle (0.5 gph and 30°) and preheated air swirled are constant for each tests . In the second test series, waste cooking oil with jet A-1 fuel-blends content of B5 and B10 with 5% and 10% respectively were burned at excess air constant at 33% ( $\phi = 0.75$ ) , while the flow rate of air was constant at 28.48 kg/hr. Radial and axial flame temperature and combustion efficiency profiles in the combustion chamber (confine tube) at different radial and axial position are discussed for the selected operating conditions The results showed that the use of mixture B5 and B10 compared to jetA-1 gave relatively lower values of gas temperature inside the flame zone. These results encourage the use of a mixtures of 5% and B10% biodiesel and Jet-A1 fuel in combustion chamber without modifications in combustion chamber design. Flame temperature distribution was recorded in all positions within the combustion chamber. Where the highest flame temperature was recorded at 3212 K using B10% biodiesel, and the highest flame temperature was recorded at 2806 K at B5 % biodiesel. The lowest flame temperature of 653 K was recorded using the combustion of B0% fuel A-1 jet.

### 1. Introduction

The increasing rates of fossil fuel consumption in all life activities may lead in the near future to the depletion of fossil fuel sources, and the increased use of fossil fuels has led to an increase in global warming, as well as to an increase in climate change rates, as well as to an increase in pollution rates and the spread of incurable and devastating diseases for human health. The intensive consumption of fossil fuels in all sectors, including the sectors of power generation, industrial processes, transportation, and others, has led to the need for extensive research to find new, renewable and environmentally friendly alternative fuels. One of the most prominent options for providing energy requirements is the use of biofuels and their mixtures with fossil fuels. If fossil fuels are limited and harmful to the environment, then biofuels are renewable, environmentally friendly and economically competitive. The general name for diesel vehicles that can be produced from edible and inedible vegetable oils, as well as animal fats, as well as edible oil waste, etc. are all called biodiesel. Biodiesel has gained significant attention due to its renewable, biodegradable, non-toxic, high cetane content, higher flash point, and lower

emission of carbon monoxide, particulate matter, unburned hydrocarbons, sulfur, and volatile organic compounds than conventional diesel [1]. There are three generations on which the classification of raw materials used in the production of diesel fuel depends, as shown in Table 1. The first generation of feedstocks used to produce biodiesel include edible oils such as soybean, rapeseed, palm, castor, etc And because the first generation relies on edible oils in the production of biodiesel, and this poses a threat to global food security, so researchers have begun to use oils derived from non-edible crops such as *Jatropha* and *Jjoba* classified as second-generation feedstocks for the production of biodiesel. One of the main advantages of using second-generation raw materials for the production of biodiesel is that it will not represent a threat to global food security, and the second-generation materials can be cultivated in non-agricultural lands in the desert and irrigated with wastewater. One of the most important problems of the second generation is the unwillingness of farmers to grow these agricultural crops. Raw materials of the third generation have addressed the difficulties and problems faced by previous generations, such as the impact on the food chain, economic feasibility and availability [2]. The use of neat biodiesel and its

blending with fossil fuels in various ratios has reduced unwanted toxic emissions such as unburned hydrocarbons (UHC) and carbon monoxide (CO) and the smoke level as it led to increased emissions such as carbon dioxide (CO<sub>2</sub>) and nitrogen oxides (NO<sub>x</sub>) [2]. Further reductions in pollutant emissions can

also be achieved with the help of combustion optimization technologies. One such technology is the Fat Free Premix (LPP) combustion. To remove all the complexities of a diffusion flame, liquid fuels are burned via premixed combustion rather than diffusion combustion.

**Table (1)** Biodiesel production from raw materials [3].

Feedstocks for biodiesel production :			
Edible oil (1st generation)		Non – edible oil (2 nd generation)	Other sources (3 rd generation)
Rapeseed oil [4, 12]		Jatropha curcus [7,14]	Waste cooking oil [9,16]
Palm oil [5 ,13]		Jojoba [8,15]	Chicken fat oil [10,15]
Castor oil [6 ,13]			Fish oil [11, 17]
Soybean oil [7 ,14]			Micro algae [11, 17]

A summary of the results of previous research is presented in Table (2). It can be concluded that there are different parameters that affect the emissions from biodiesel combustion. Some of these parameters such as the high viscosity of biodiesel increase carbon dioxide emissions while other parameters such as the oxygen content of biodiesel tend to reduce these emissions and temperature increase.

**Table (2)** Emissions from the combustion of biodiesel in boilers and testing combustors.

Ref.	Biodiesel type	T	CO	UHC	NO <sub>x</sub>
• El-Zoheiry [18]	Jojoba oil biodiesel-Jet-A1 blends	Decrease	Increase	Increase	Decrease
Belal [19]	Waste cooking oil methyl ester and Jet A-1	Decrease	Increase	-----	Decrease
Attia [20]	(WCOME) with Jet A-1 (symbolized as B5, B10, B15, and B20)	Increase: at (B20)	Decrease : at (B20)	-----	Decrease : at (B20)
Jr [21]	Canola methyl ester	Decrease		-----	Decrease
San José [22]	Sunflower oil biodiesel	Increase	Decrease	-----	-----
Ghorbani [23]	Soybean and Sunflower oils	Decrease	Increase	-----	Decrease
Ng [24]	Pome	Increase	Decrease	-----	Increase
Panchasara [25]	Soybean and animal fat oils	Increase	Decrease	-----	Decrease

The possibility of using any alternative fuel in aircraft gas turbines and any other combustion system depends on the characteristics of fuel combustion and the harmful effects on the environment [26]. The technology that contributes to achieving the best combustion quality with minimal toxic emissions is the combustion method (LPP).

## 2.The Main Components of Test Rig:

As can be seen from fig. (1), the test rig consists of the following main components:

1. Prevaporized fuel line.
2. A stage of heating air supply.
3. A stage of swirl burner.
4. A stage of confined tube and exhaust gaseous.

The following subsections give more details about these systems.

Referring to fig. (1), the combustor comprises the two pipes of progressively larger diameter. These pipes referred to the swirl burner and confined tube. These pipes may be mounted in a conventional manner, the overlapping substantially concentric alignment of the pipes defined a central passage and annular passages. Each of the central and annular passages respectively defined a central intake opening and annular intake openings formed at the end of exhaust confined tube .Swirl burner serve to form flow enveloped including toroidal vortices.

The diameter ratio of swirl burner and confined tube is:  $D_b/D_c = 0.3$  and length of confined tube is:  $L_c = 500$  mm .

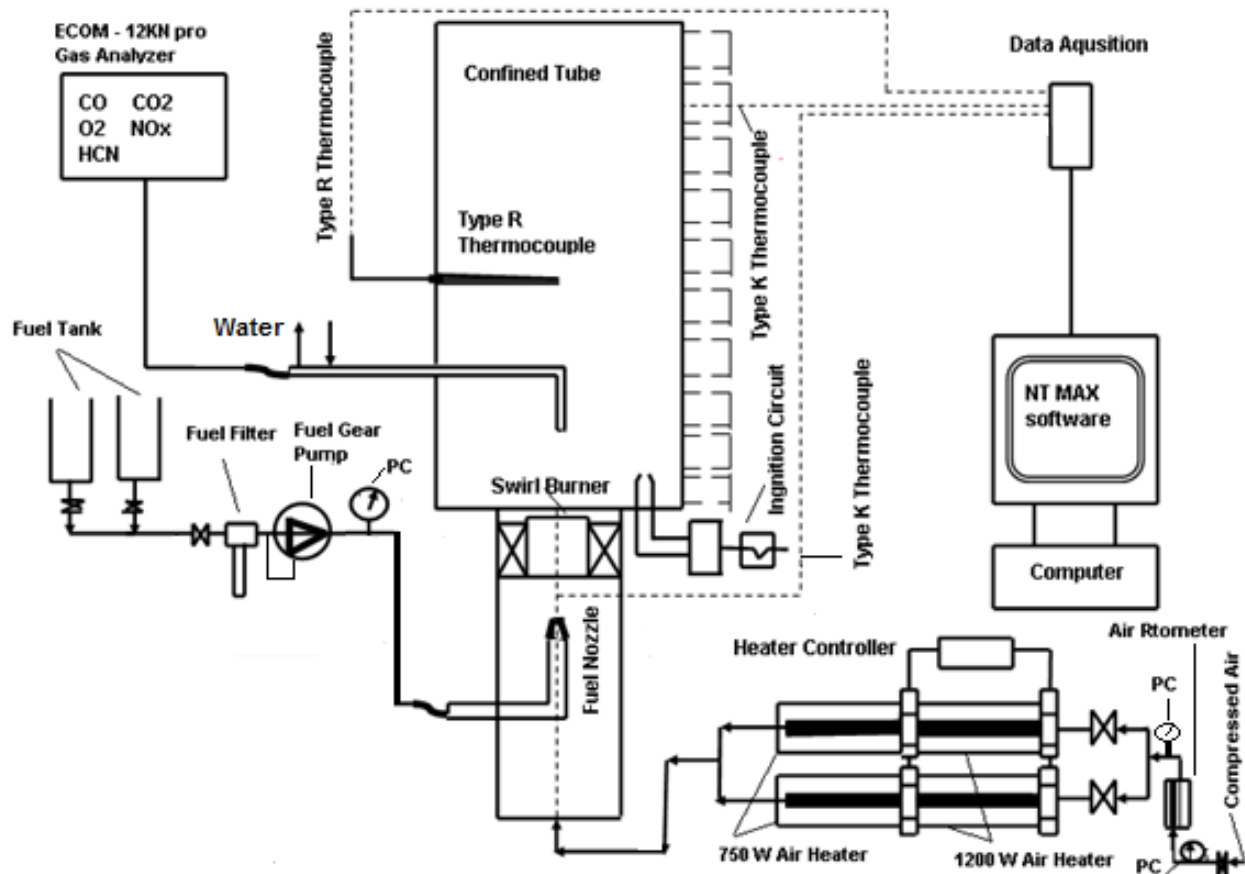


Figure (1) Test rig schematic drawings

### 3. Results and discussion

The experimental results of the combustion tests are based on the combustion characteristics of the fuels tested using a lean premixed prevaporized combustion test facility are presented. The results are analyzed and discussed in comparison with similar results cited in the literature. Series of experiments were conducted to measure the temperature with different values of fuel blending ratio BR (B0, B5 and B10), and with constant values of equivalence ratio ( $\Phi_{\text{overall}} = 0.75$ ), constant values of air flow rate (28.48 kg/hr) at air preheating temperature (250 °C), constant values of fuel flow rate  $m_{\text{fuel}} = 1.471 \text{ kg/hr}$  at (B0),  $m_{\text{fuel}} = 1.477 \text{ kg/hr}$  at (B5) and  $m_{\text{fuel}} = 1.498 \text{ kg/hr}$  at (B10). Also, the temperature distribution along the radial axis ( $r/R\%$ ) and vertical axis ( $x/X\%$ ) of the combustor (or confine) for different blending ratio and constant equivalence ratio, type R(Pt/Pt-Rh13%) thermocouple used to measure flame temperatures. The effect of blending ratio BR (B0, B5 and B10) on the flame temperature distribution along the different location of combustion zones was also studied.

#### 3.1. Flame Temperature Distribution :

Concentration of waste cooking oil (WCO) in B5 is 95% WCO and in B10 90% WCO, the boiling point temperature of waste cooking oil (WCO) is 350 °C,

the boiling point temperature of fuel jet-A1 (B0) is 163 °C and preheated air temperature is 250 °C. Then concentration of liquid vapor from prevaporized of fuel jet-A1 is greater than B5 and B10, and concentration of liquid vapor from prevaporized of B5 is greater than B10 ( $B0 > B5 > B10$ ). Then, burning of B0 is faster than B5 and B10, also burning of B5 is faster than B10. And also, heating value of fuel jet-A1 (B0) is (43.463 kJ/kg) is greater than heating value of waste cooking oil (WCO) (39.98 kJ/kg), heating value of  $B0 > B5 > B10$ . And also, viscosity of fuel jet-A1 (B0) is (1.08 cSt) is lower than waste cooking oil (WCO) (4.53 cSt), viscosity turbulence of (WCO) is higher than viscosity turbulence of fuel jet-A1, viscosity turbulence of  $B10 > B5 > B0$ , intensity turbulence of  $B0 > B5 > B10$ . And also, toroidal reversal flow which created from the swirler existed at the tip burner serve to form flame cavities in the flame zones, flame cavities includes some of liquid vapor as in case of B0 and include liquid droplets as in cases of B5 and B10, and also flame temperature becomes maximum in cases of B5 and B10 rather than of B0 where the oxidant and liquid vapor of B5 and B10 prevaporized are react stoichiometrically. And also, oxygen content of (WCO) (11.3 % by mass) is higher than fuel jet-A1 (B0) (Nil), oxygen content of  $B10 > B5 > B0$ . And also, Molecular

weight of fuel jet-A1 (B0) is (148.025 kg/kmol) is lower than waste cooking oil (WCO) (290.914 kg/kmol) . Figures (4-14) show a higher level of similarity between flame temperature B0, B5, and B10.

in contour figures (4,5 and 6); These curves indicate a decrease in the flame temperature when increasing ( $r/R$  %) from the burner central radius to the outer radius of the burner, until ( $r/R = 78.74\%$ ), temperature reaches a minimum value. It is worth noting that the local equivalence ratio ( $\Phi_{local}$ ) achieves its lean value at  $r/R = 78$  %. Also. The vortices resulting from the swirl burner create angular momentum, and this angular momentum assists in the combustion of waste cooking oil droplets at the outer radius of the burner away from the center line of the burner as rich mixture. The flame temperatures also decrease with increase in axial distance ( $x/X$ %) from the central axial of the tip burner to the outlet end of the exit burner, until axial distance ( $x/X = 48$  % - 98%), temperature reaches a minimum value. It is worth noting that the local equivalence ratio ( $\Phi_{local}$ ) achieves its lean value at  $x/X = 48$  % - 98%. The curves also indicated that the flame temperature increases with decrease in radial distance ( $r/R$ %) and decrease in axial distance ( $x/x$ %) of the burner , until ( $r/R = 0$  and  $x/x = 0$ ), temperature reaches a peak value . It is worth noting that the flame cavities created by the swirler includes some liquid droplets or vapors, Because of the vortices resulting from the swirl burner, spherical symmetrical flame cavities are formed. These cavities flames include some of liquid droplets as in cases of (B5 and B10) and includes some of liquid droplets as in case of B0, and the flame temperature becomes maximum.

Figures (7-10) are plotted for B0, B5 and B10 and equivalence ratio 0.75. The temperature decreases by increasing radial axis  $r/R$ %. It is worth noting that the local equivalence ratio ( $\Phi_{local}$ ) achieves its lean value at  $r/R = 78$  %.

Figures (7-10) are plotted for B0, B5 and B10 and equivalence ratio 0.75. The peak temperature for each blend occurs at radial axis  $r/R = 0$ . It is worth noting that the flame cavities created by the swirler includes some of liquid droplets or vapors.

Figures (11-14) are plotted for B0, B5 and B10. The temperature increases in these figures (12-14) by increasing the axial distance ( $x/X$ %) until a peak value at a certain value (as shown in these figs) after these peaks the temperature decreases by increasing the axial distance  $x/X$  % . It is worth noting that the local equivalence ratio ( $\Phi_{local}$ ) achieves its stoichiometric value at  $x/X = (10\%-40\%)$

respectively , As shown in the figures with colored lines . The value of  $x/X$  % at which the peak temperature occurs varies with changes in fuel blending ratios (B0 ,B5 and B10) or in local equivalence ratio .It is worth – mentioning that for each one blending ratio (B0, B5 and B10) , the local zone becomes stoichiometric when the following relations are satisfied :  $\Phi_{local} = \Phi_{stoich}$  . These curves also showed a difference in all temperature values and also in the positions ( $x/X$ %) of the peak temperature for B0, B5 and B10. The lag of the peak temperatures for both B5 and B10 blends than for B0 blend; in case of B5 and B10, bigger of waste cooking oil droplets, high density , high boiling point temperature and high viscosity of waste cooking oil due to decrease velocity burning and increase evaporation time, shear layer interaction of intensity turbulence of B5 and B10 is lower than B0 and take more burning velocity. The flame temperature of burning B10 is greater than B5 or B0 , as in figs (7-14) , a shear layers interaction of viscosity turbulences of B10 is greater than B5 and B0 as shown in fig.(2) , and oxygen content of B10 is greater than B5 and B0 due to reaction rate of B10 is greater than B5 and B0. The flame temperature of B5 is greater than B10 or B0, as in figs (7-9 and 11-14) , a shear layers interaction of viscosity turbulences of B5 is greater than B0 , and oxygen content of B5 is greater than B0 , due to reaction rate of B5 is greater than B0. And a shear layers interaction of intensity turbulences of B5 is greater than B10, and heating value of B5 is greater than B10.

As in case of B5 and B10, a shear layers interaction of viscosity turbulences and flame cavities are formed in flame zones serve to form flame stability, and the flame temperature becomes maximum as shown in figs (4-14).

There are higher levels of similarity between the flame temperature of B0 ,B5 and B10 at ( $x/X = 0.98$ ), and this is shown by the figures (11-14).The heterogeneity of all the results of the combustion process is also due to the heterogeneity of the mixing process, as well as the inhomogeneity of the thermal, physical and physicochemical properties of burning of the fuel and biofuel blends (B0 ,B5 and B10).

In cases of B5 and B10, there are three different reactions for each case as the following; (a) A shear layers interaction between two liquid droplets, (b) A shear layers interaction between liquid droplets and liquid vapor and (c) A shear layers interaction between two liquid vapors .In case of B0 . there is a shear layer interaction between two liquid vapors, (As shown in fig.2).

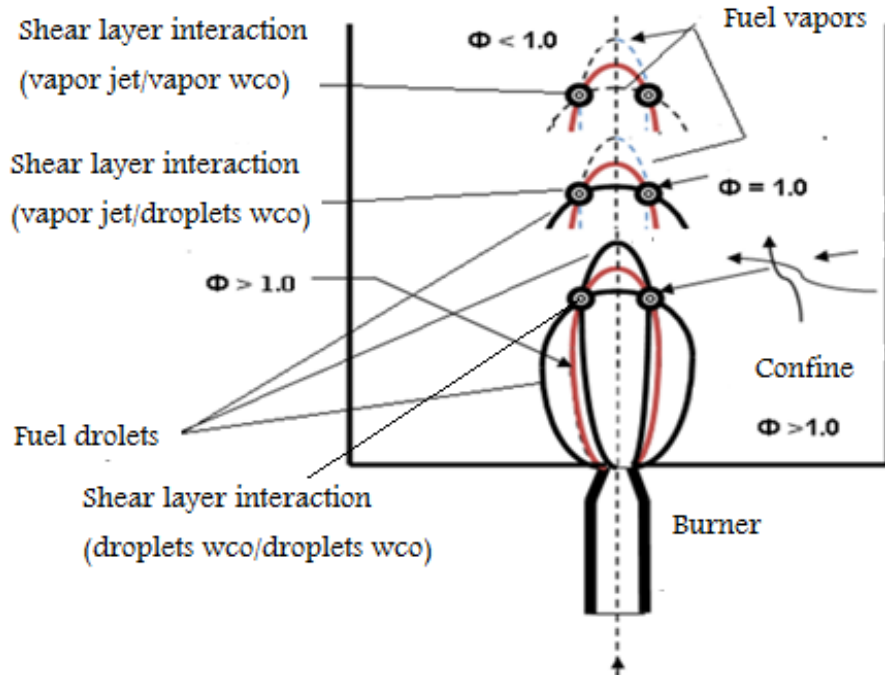


Figure (2) Flame structure into different locals combustion.

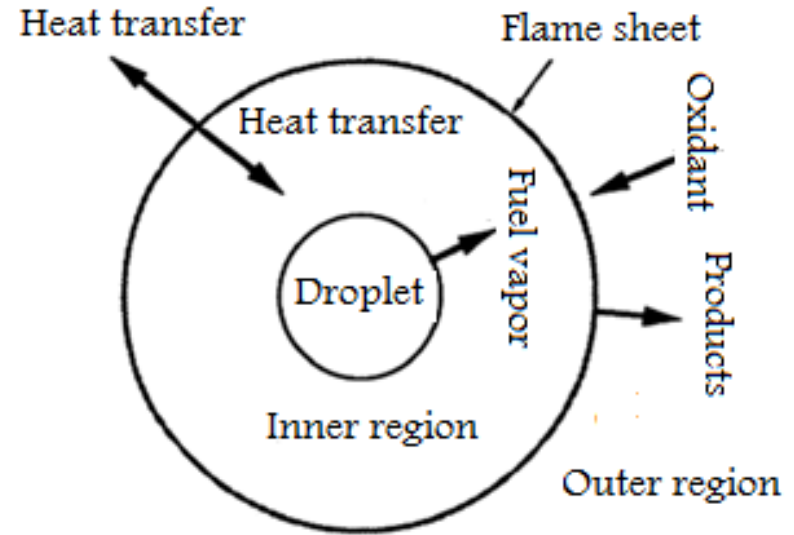


Figure (3) Burning a droplet of fuel inside oxidizing flame cavities

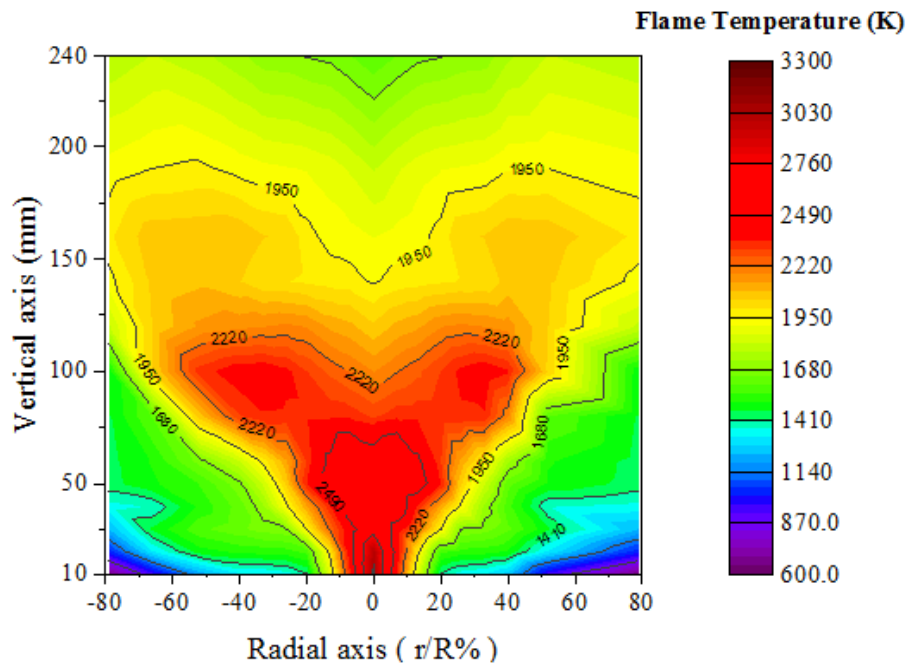


Fig.(4): Contoure of the flame temperature (k) distribution along the radial and vertical axis for ;B0 at  $\Phi(\text{overall})=0.75$  .

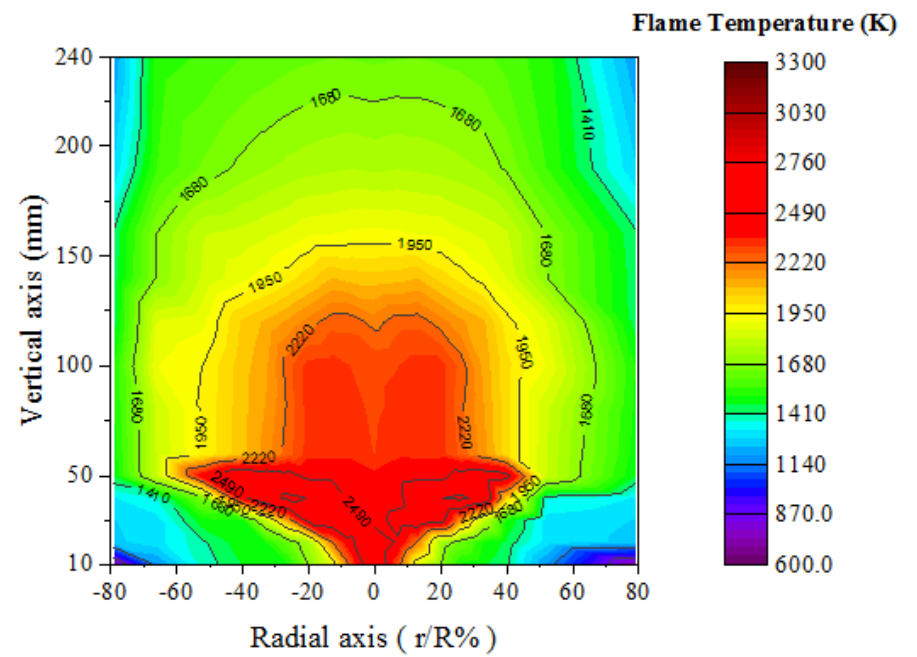


Fig.(5): Contoure of the flame temperature (k) distribution along the radial and vertical axis for ; B5 at  $\Phi(\text{overall})=0.75$  .

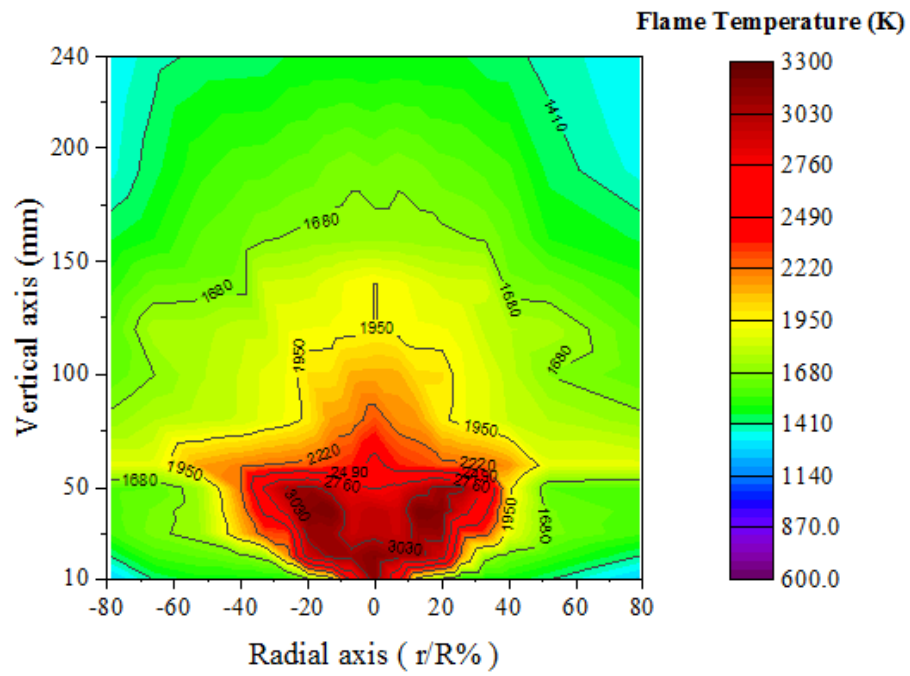


Fig.(6): Contoure of the flame temperature (k) distribution along the radial and vertical axis for ;B10 at  $\Phi(\text{overall})=0.75$  .

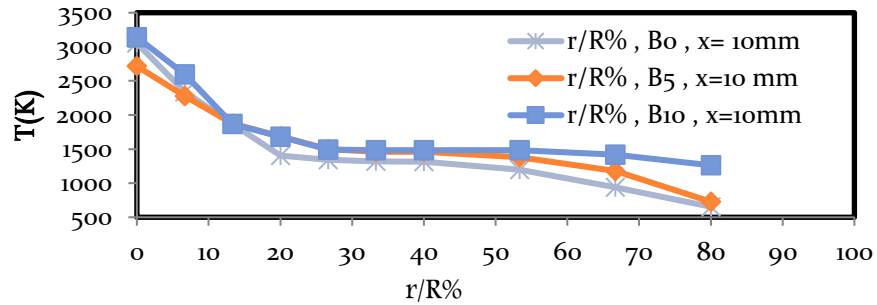


Fig. ( 7 ) B0 , B5 and B10 radial distribution flame temperature measurements at  $\Phi_{\text{overall}} = 0.75$  and  $x = 10\text{mm}$ .

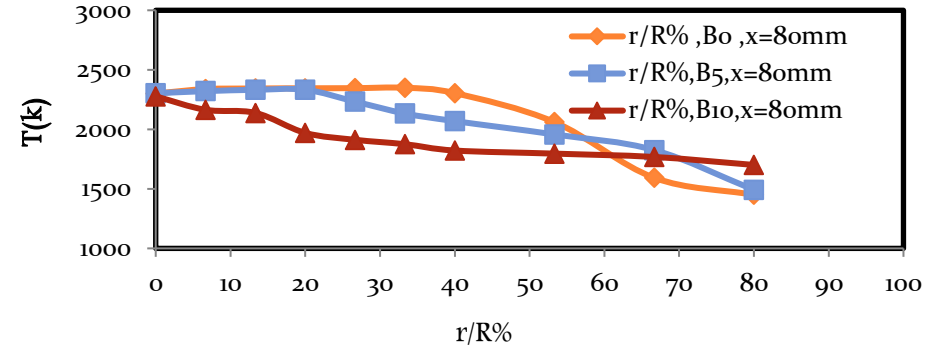


Fig. (8) B0 , B5 and B10 radial distribution flame temperature measurements at  $\Phi_{\text{overall}} = 0.75$  and  $x = 80\text{mm}$ .

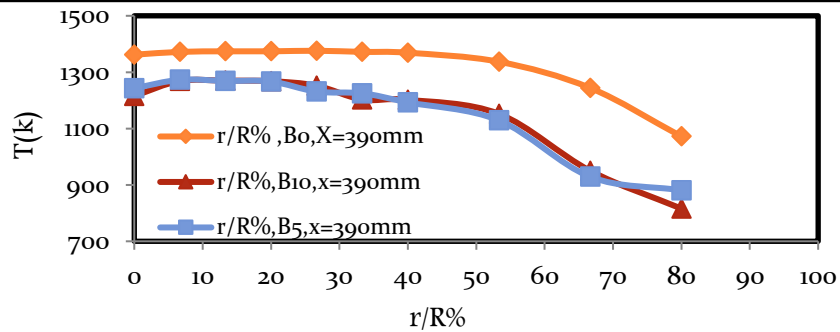


Fig. (9) B0 , B5 and B10 radial distribution flame temperature measurements at  $\Phi_{\text{overall}} = 0.75$  and  $x = 390\text{mm}$ .

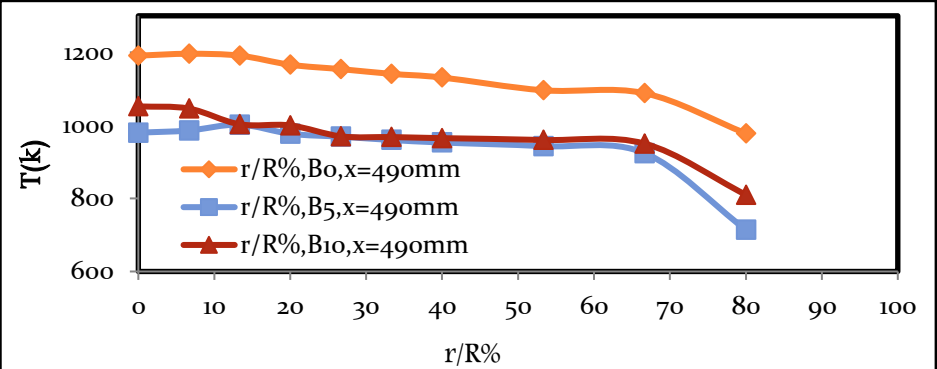


Fig. (10) B0 , B5 and B10 radial distribution flame temperature measurements at  $\Phi_{\text{overall}} = 0.75$  and  $x = 490\text{mm}$ .



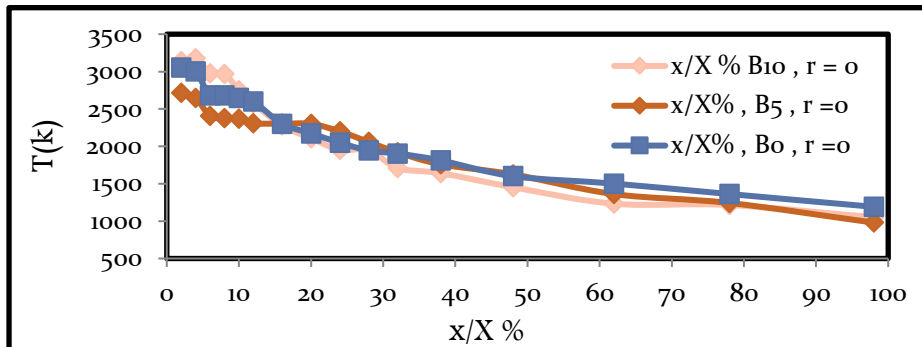


Fig. ( 11)B0 , B5 and B10 axial distribution flame temperature measurements at  $\Phi_{\text{overall}} = 0.75$  and  $r = 0$ .

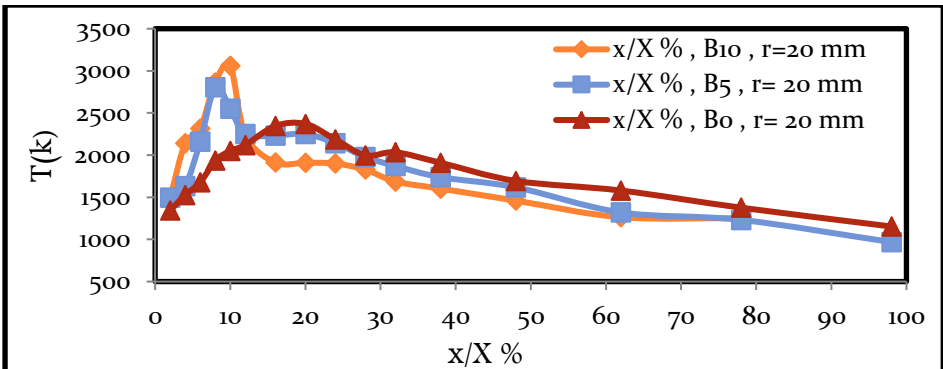


Fig.(12)B0 , B5 and B10 axial distribution flame temperature measurements at  $\Phi_{\text{overall}} = 0.75$  and  $r = 20 \text{ mm}$ .

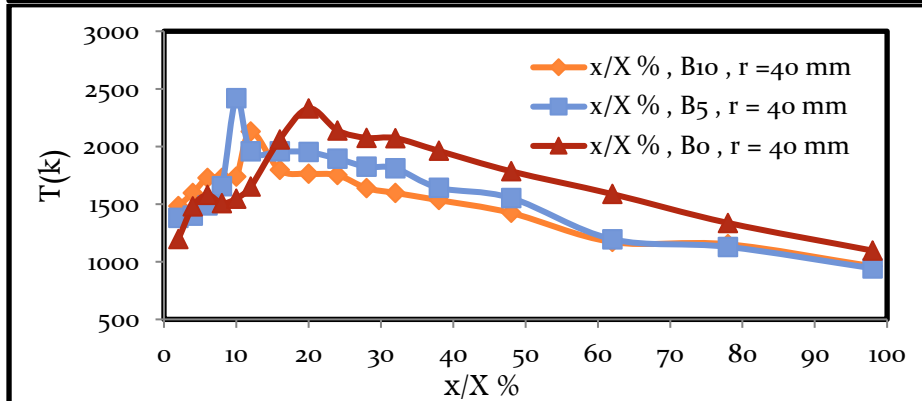


Fig.(13)B0 , B5 and B10 axial distribution flame temperature measurements at  $\Phi_{\text{overall}} = 0.75$  and  $r = 40 \text{ mm}$ .

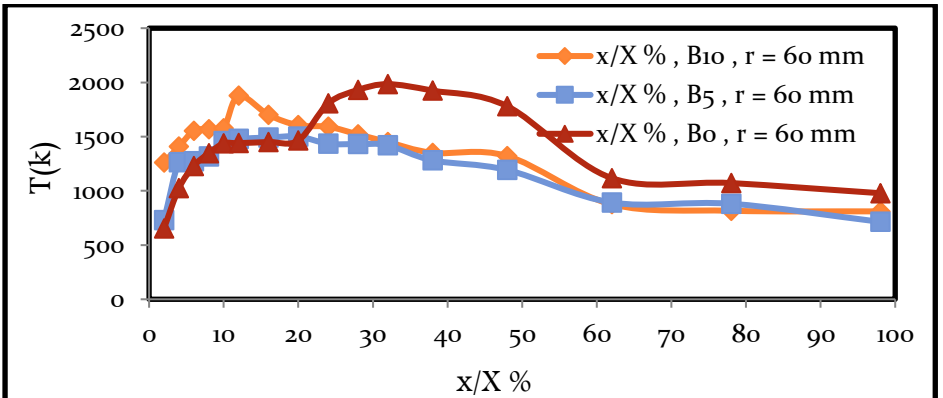


Fig. (14)B0 , B5 and B10 axial distribution flame temperature measurements at  $\Phi_{\text{overall}} = 0.75$  and  $r = 60 \text{ mm}$ .

#### 4. Conclusions

The study showed the effect of the blending ratio of biodiesel on the combustion characteristics of jet fuel using pre-mixed prevaporized combustion technique. Biodiesel was produced from waste crude cooking oil by a cross-conversion process including conversion of wco to wco methyl ester (WCOME). The combustion technology of the base fuel is mainly mixed under lean conditions to achieve the highest thermal combustion efficiency and flame temperature.

This study achieved three objectives, the first objective is to produce biodiesel from waste cooking oil (WCO) using the best conditions for the transesterification process. The second objective is to evaluate the combustion characteristics of fuel jet and jet fuel mixture in a lean pre-vaporized combustor under the same conditions. The third objective is to evaluate the combustion characteristics of WCOME-jet-A1 blended fuels in a lean premixed prevaporized combustor under the same conditions. From the results of the study, the following groups of conclusions can be obtained.

##### 4.1. Concluding Remarks

Main conclusions that can be extracted from the present work are summarized below :

1. Flame stabilization were achieved for all experimental the current work , this results due to shear layers interaction of viscosity turbulences and flame cavities which are formed in different flame zones .
2. The flame temperature becomes maximum at different zones ( $T = 3212\text{K}$  at B10),
3. Temperature variation in the flame zone with the radial and horizontal distance results from the following:
  1. Generation of different shear layer interaction at different locations in the flame zones, such as:
    - a Shear layer interaction between two liquid droplets,
    - b- Shear layer interaction between two liquid vapors,
    - c. Shear layer interaction between liquid droplets and liquid vapor.
  4. Generation of different local equivalence ratios at different locations in the flame zones, such as:
    - a local rich mixture,
    - b. Local Stoichiometric,
    - c. Local lean mixture.
  5. Generation of different flame cavities at different locations in the flame zone.
  6. Generation of high turbulence intensity.
  7. Different effect of viscosity turbulence on blending ratio B5, B10 and fuel jet (B0).
  - 9.
  10. Local equivalence ratio ( $\Phi_{\text{local}}$ ), the overall one plays a significant role. Increasing in the value of this local equivalence ( $\Phi_{\text{local}} \geq 0.75$ ) approaches to stoichiometric causes increasing in temperature (653k to 3212 k).

##### 4.2. Recommendations for Future Work

Further research work can be made in order to pursue the present thesis. This research work is summarized as follows: -

1. Investigate the heat transfer from the WCOME-jet-A1 fuel flames in the LPP combustor to help in the combustor design.
2. Investigate the effect of increasing preheating air temperature over  $250\text{ }^{\circ}\text{C}$  on the prevaporization of the Jet-A1, blending mixture of the WCOME -Jet-A1, combustion characteristics of the WCOME-jet-A1 fuel combustion to obtain the best combustion efficiency and the best configuration of turbulent flames and further reduction in the emissions and more flame stability.
3. Studying the effect of swirl numbers on exit temperature and thermal combustion efficiency.
4. Extensive study of the effect of the distribution pattern of air staging on exit temperature and thermal combustion efficiency.
5. Studying the effect of  $m_f$  and excess air on exit temperature and thermal combustion efficiency.
6. Studying the performance of the present combustor design using different fuels , such as kerosene , diesel fuels , natural gas or biodiesel (Such as ; Soybean , PME , Straight vegetable oil , Recycled cooking oil , Castor , Soybean and Palm , Soy , canola and recycled rapeseed methyl ester and hog - fat biofuel , fish , vegetable and bio oil FAME).
7. Extensive study of the effect different values of equivalence ratio ( $\Phi$ ) on exit temperature, thermal combustion efficiency and flame stability
8. Extensive study of the effect different percentage of blending ratios, such as B15 , B20 , B25 and B30 on exit temperature , thermal combustion efficiency and flame stability .

##### References

- [1] Kumar, R.S., Sureshkumar, K., & Velraj, R. (2015). Optimization of biodiesel production from Manilkara zapota (L.) seed oil using Taguchi method. *Fuel*, 140, 90-96.
- [2] Sakthivel, R., Ramesh, K., Purnachandran, R., & Shameer, P. M. (2018). A review on the properties, performance and emission aspects of the third generation biodiesels. *Renewable and Sustainable Energy Reviews*, 82, 2970-2992.
- [3] Habib, Z., Parthasarathy, R., & Gollahalli, S. (2010). Performance and emission characteristics of biofuel in a small-scale gas turbine engine. *Applied Energy*, 87(5), 1701-1709.
- [4] H.K. VERSTEEG and W. MALALASEKERA, "An introduction to computational fluid dynamics The finite volume Method ", 2009 , Longman Scientific & Technical.
- [5] Bertrand P.A.M., Andrade M.H., Luijten C.C.M., Goey L.P.H. Soot formation of lignin derived fuels in a laminar co-flow diffusion flame,

- M.Sc. Thesis, Technics University Eindhoven, Department of Mechanical Engineering, Section Combustion Technology, July 2009 .
- [6] Salvi B.L., Panwar N.L. Biodiesel resources and production technologies – A review. *Renewable and Sustainable Energy Reviews* 2012; 16:3680– 3689.
- [7] Demirbas A. Political, economic and environmental impacts of biofuels: A review. *Applied Energy* 2009; 86:S108–S117.
- [8] Abbaszaadeh A., Ghobadian B., Omidkhah M. R., Najafi G. Current biodiesel production technologies: A comparative review. *Energy Conversion and Management* 2012; 63:138–148.
- [9] Bankovic-Ilic I. B., Stamenkovic O. S., Veljkovic V. B. Biodiesel production from non-edible plant oils. *Renewable and Sustainable Energy Reviews* 2012, 16: 3621-3647.
- [10] Atabani A.E., Mahlia T.M.I., Masjuki H.H., Badruddin I. A. A comparative evaluation of physical and chemical properties of biodiesel synthesized from edible and non-edible oils and study on the effect of biodiesel blending. *Energy* 2013; 58: 296-304.
- [11] Atabani A.E., Silitonga A.S., Badruddina I. A., Mahlia M. I., Masjuki H. H., Mekhilef S. A comprehensive review on biodiesel as an alternative energy resource and its characteristics. *Renewable and Sustainable Energy Reviews*, 2012; 16: 2070-2093.
- [12] Pinto C. D. G., Varanda Coutinho J. M. A. P., Oliveira N. S., Ferreira I. M. D. J. M. Thermal conductivity of gas mixtures for polyurethane rigid foams. M.Sc. thesis. University of Aveiro, Department of Chemistry 2009.
- [13] Poling B. E., Prausnitz J. M., O'Connell J. P. The properties of gases and liquids. Fifth edition. By McGraw-Hill 2001.
- [14] Louro C. S. C., Ismael M. R. C., Gil M. G. S. B., Dohrn R., Fareleira J. M. N. A. Thermal conductivity of gases: transient hot-wire method. M.Sc. Thesis. Technical University of Lisbon 2008.
- [15] Gui M.M., Lee K.T., Bhatia S. , "Feasibility of edible oil vs. non-edible oil vs. waste edible oil As Biodiesel feedstock", *Energy* 2008; 33: 1646– 1653.
- [16] Singhabhandhu, A. and Tezuka, T., "Prospective framework for collection and exploitation of waste cooking oil as feedstock for energy conversion", *Energy*, 35 (4), 1839 (2010).
- [17] H. M. A. Khalil, " Numerical Investigation of Flameless Combustion in Gas Turbine - Applications", Mechanical power Engineering Department , Faculty of Engineering , Alexandria University , (2018).
- [18] R. M. A. Elzoheiry, " Investigation of Combustion Characteristics for Pre-vaporized Premixed Biofuel-Jet Mixtures", Mechanical Engineering Department, Benha faculty of Engineering , Benha University , 2014:
- [19] B.Y. I. Belal, " Investigation of Stabilized Flame for Lean Premixed and Pre-vaporized Biofuel Combustion", Mechanical Engineering Department, Benha faculty of Engineering , Benha University , 2018:
- [20] Attia, A. M., El-Zoheiry, R. M., El-Batsh, H. M., & Shehata, M. S. (2014, November). Combustion Characteristics of Jojoba Methyl Ester as an Alternative Fuel for Gas Turbine. In ASME 2014 International Mechanical Engineering Congress and Exposition. American Society of Mechanical Engineers.
- [21] Jr. J. A. E., Parthasarathy R., Gollahalli S. Atomization and combustion of canola methyl ester biofuel spray. *Fuel* 2010; 89: 3735–3741.
- [22] San José J., Al-Kassir Awf, Sastre J.A. y López, Gañán J. Analysis of biodiesel combustion in a boiler with a pressure operated mechanical pulverisation burner. *Fuel Processing Technology* 2011; 92: 271–277. 121
- [23] Ghorbani A., Bazooyar B., Shariati A., Jokar S. M., Ajami H., Naderi A.. A comparative study of combustion performance and emission of biodiesel blends and diesel in an experimental boiler. *Applied Energy* 2011; 88: 4725–4732.
- [24] Ng H. K., Gan S. Combustion performance and exhaust emissions from the non-pressurized combustion of palm oil biodiesel blends. *Applied Thermal Engineering* 2010; 30: 2476-2484.
- [25] Panchasara H. V., Simmons B. M., Agrawal A. K. Combustion performance of biodiesel and diesel-vegetable oil blends in a simulated gas turbine burner. *ASME* 2008; GT2008-51496.
- [26] Yi J., Xiaomin H., Jingyu Z., Bo J., Zejun W. Experimental study on emission performance of an LPP/TVC. *Chinese Journal of Aeronautics* 2012; 25: 335-341.